

# Exoribonuclease R Interacts with Endoribonuclease E and an RNA Helicase in the Psychrotrophic Bacterium *Pseudomonas syringae* Lz4W\*

Received for publication, December 1, 2004, and in revised form, February 4, 2005  
Published, JBC Papers in Press, February 10, 2005, DOI 10.1074/jbc.M413507200

Rajyaguru Ichchhashankar Purusharth<sup>‡§</sup>, Franziska Klein<sup>¶</sup>, Shaheen Sulthana<sup>¶||</sup>,  
Stephanie Jäger<sup>¶</sup>, Medicharla Venkata Jagannadham<sup>‡</sup>, Elena Evguenieva-Hackenberg<sup>¶</sup>,  
Malay Kumar Ray<sup>‡\*\*</sup>, and Gabriele Klug<sup>¶‡‡</sup>

From the <sup>¶</sup>Institut für Mikrobiologie und Molekularbiologie der Justus-Liebig-Universität Giessen, Heinrich-Buff-Ring 26-32, 35392 Giessen, Germany and the <sup>‡</sup>Centre for Cellular and Molecular Biology, Uppal Road, Hyderabad 500007, India

Endoribonuclease E, a key enzyme involved in RNA decay and processing in bacteria, organizes a protein complex called degradosome. In *Escherichia coli*, *Rhodobacter capsulatus*, and *Streptomyces coelicolor*, RNase E interacts with the phosphate-dependent exoribonuclease polynucleotide phosphorylase, DEAD-box helicase(s), and additional factors in an RNA-degrading complex. To characterize the degradosome of the psychrotrophic bacterium *Pseudomonas syringae* Lz4W, RNase E was enriched by cation exchange chromatography and fractionation in a glycerol density gradient. Most surprisingly, the hydrolytic exoribonuclease RNase R was found to co-purify with RNase E. Co-immunoprecipitation and Ni<sup>2+</sup>-affinity pull-down experiments confirmed the specific interaction between RNase R and RNase E. Additionally, the DEAD-box helicase RhlE was identified as part of this protein complex. Fractions comprising the three proteins showed RNase E and RNase R activity and efficiently degraded a synthetic stem-loop containing RNA in the presence of ATP. The unexpected association of RNase R with RNase E and RhlE in an RNA-degrading complex indicates that the cold-adapted *P. syringae* has a degradosome of novel structure. The identification of RNase R instead of polynucleotide phosphorylase in this complex underlines the importance of the interaction between endo- and exoribonucleases for the bacterial RNA metabolism. The physical association of RNase E with an exoribonuclease and an RNA helicase apparently is a common theme in the composition of bacterial RNA-degrading complexes.

RNA maturation and degradation involve the action of different ribonucleases, some of which are organized in protein complexes. It is reasonable to assume that such complexes

work like molecular machines and would therefore catalyze different enzymatic steps in an ordered manner. *Escherichia coli* possesses an RNA-degrading complex called degradosome. It is organized by the endoribonuclease RNase E, which is tightly associated with the exoribonuclease polynucleotide phosphorylase (PNPase),<sup>1</sup> the DEAD-box helicase RhlB, and enolase (1–3). Polynucleotide kinase, poly(A) polymerase, and the chaperones DnaK and GroEL are also implicated to be components of this complex (4–7). The existence of the *E. coli* degradosome *in vivo* and its roles in mRNA and rRNA degradation are well documented (8–10). RNase E organizes the degradosome via its C-terminal protein binding scaffold, whereas its catalytic domain is located in the N-terminal part (11).

Not all bacteria have a gene for RNase E (*rne*), and some bacteria possess only short RNase E homologues without potential protein binding domains (12). They most probably do not harbor degradosomes. The remaining species with long RNase E versions are thought to have degradosomes, the structure of which may differ from that of *E. coli*. The second bacterial RNase E-based protein complex studied was that of *Rhodobacter capsulatus* (13). RNase E of *R. capsulatus* strongly interacts with a DEAD-box helicase, the transcription termination factor Rho, and two other previously unidentified proteins. A second DEAD-box helicase also co-purifies with *R. capsulatus* RNase E. PNPase is not tightly associated with the complex but is found in substoichiometric amounts in RNase E-containing fractions after three purification steps (13). Recently, it was shown that a structurally shuffled RNase E homologue in *Streptomyces coelicolor* harbors its active center in the middle of the molecule and interacts with PNPase via its N-terminal part (12). The available data imply that the bacterial degradosome consists of RNase E, DEAD-box helicase(s), the phosphate-dependent exoribonuclease PNPase, and additional subunits, which vary in the different species. Each monomer of the homotrimeric PNPase harbors two RNase PH-like domains (RNase PH, EC 2.7.7.56). The six RNase PH-like domains of PNPase are organized in a ring, similarly to the six RNase PH-like domain-containing subunits of the eukaryotic RNA-processing and -degrading complex, the exosome (14, 15). The structural similarity between PNPase and the exosome ring led to the suggestion that the RNA-degrading complexes of bacteria and eukaryotes may have functional similarities and/or a common evolutionary origin. It was shown that the archaeon *Sulfolobus solfataricus* possesses

\* This work was supported in part by the Volkswagen Foundation. The costs of publication of this article were defrayed in part by the payment of page charges. This article must therefore be hereby marked "advertisement" in accordance with 18 U.S.C. Section 1734 solely to indicate this fact.

§ Recipient of a senior research fellowship from Council of Scientific and Industrial Research (CSIR), India.

¶ Recipient of a junior research fellowship from CSIR, India.

\*\* To whom correspondence may be addressed: Centre for Cellular and Molecular Biology, Hyderabad 500007, India. Tel.: 91-40-27192512; Fax: 91-40-27160591; E-mail: malay@cemb.res.in.

‡‡ To whom correspondence may be addressed: Institut für Mikrobiologie und Molekularbiologie, Heinrich-Buff-Ring 26-32, 35392 Giessen, Germany. Tel.: 49-641-99-35542; Fax: 49-641-99-35549; E-mail: Gabriele.Klug@mikro.bio.uni-giessen.de.

<sup>1</sup> The abbreviations used are: PNPase, polynucleotide phosphorylase; Ni-NTA, nickel-nitrilotriacetic acid; PAP, poly(A) polymerase.

an exosome-like protein complex (16), and the existence of the exosome in many Archaea was predicted (17).

Physiologically, RNases are important virulence factors of pathogenic bacteria (18–21) and might have a role in the adaptation to different environments. For example, the exoribonucleases PNPase and RNase R accumulate under cold shock in mesophilic *E. coli* (22, 23). However, little is known about the RNA processing and degradation in psychrotrophic bacteria, some of which are pathogens. Therefore, we decided to study the degradosome of the Antarctic bacterium *Pseudomonas syringae* Lz4W, a model organism, which grows well at 4 °C (24). Most surprisingly, we found that RNase E of this strain interacts with the hydrolytic exoribonuclease RNase R in a protein complex. Another component of the complex is the DEAD-box helicase RhIE. Our data reveal the existence of a bacterial RNA-degrading complex of unexpected structure.

#### MATERIALS AND METHODS

**Bacterial Strains**—The psychrotrophic *P. syringae* Lz4W was grown at 22 or 4 °C in Antarctic Bacterial Medium composed of 5 g liter<sup>-1</sup> peptone and 2.5 g liter<sup>-1</sup> yeast extract as described earlier (24). When necessary, the culture was incubated for 2 h at 37 °C prior to harvesting. Cells were harvested at OD<sub>600</sub> of 1.0. *E. coli* strains DH5 $\alpha$  and BL21(DE3) were cultured at 37 °C in Luria-Bertani medium (LB), *E. coli* JM 109 in standard I medium (Merck). When necessary, the growth medium was supplemented with ampicillin (100  $\mu$ g ml<sup>-1</sup>), kanamycin (50  $\mu$ g ml<sup>-1</sup>), or tetracycline (20  $\mu$ g ml<sup>-1</sup>).

**Protein Fractionation**—RNase E-containing fractions of *P. syringae* Lz4W and *E. coli* JM 109 were isolated as described for the *R. capsulatus* degradosomes (13). Briefly, the 100,000  $\times$  g supernatant fraction of cell lysates was subjected to ammonium sulfate precipitation and chromatography on a sulfopropyl (SP)-Sephacrose cation exchanger column (Amersham Biosciences), which was equilibrated in buffer A containing 10 mM Tris-HCl, pH 7.5, 5% glycerol, 0.5% Genapol X-080, 1 mM EDTA, 0.1 mM dithiothreitol, 0.1 mM phenylmethylsulfonfyl fluoride, 50 mM NaCl (13). After washing with the same buffer containing first 50 and then 300 mM NaCl, RNase E was eluted with 1 M NaCl. The SP-Sephacrose fractions containing RNase E were layered on top of a 10–30% (w/v) glycerol gradient containing buffer A with 300 mM NaCl. A control experiment with the RNase A-treated SP fraction was also performed. Centrifugation was performed in a Beckman SW60 rotor at 4 °C for 21 h 30 min at 30,000 rpm. For calibration, bovine serum albumin (67 kDa), aldolase (158 kDa), catalase (240 kDa), and ferritin (440 kDa) (Amersham Biosciences) were used. Aliquots of 260  $\mu$ l (total 16 fractions) were harvested from the top of the gradient. The distribution of proteins was visualized by running aliquots of each fraction on denaturing 8–10% polyacrylamide gels with subsequent silver staining.

**Protein Sequencing and Identification**—Proteins were separated by SDS-PAGE, transferred to polyvinylidene difluoride membrane, and stained with Ponceau S reagent. The stained bands were excised, washed 10 times with MilliQ water in microcentrifuge tube, and stored at –30 °C. The strips were used for N-terminal amino acid sequencing by the Edman degradation method on an Automated Protein Sequencer Procise cLC from Applied Biosystems. The N-terminal sequence was used for Protein Blast analysis at NCBI ([www.ncbi.nlm.nih.gov](http://www.ncbi.nlm.nih.gov)) using the default parameters of search for short, nearly exact matches. The proteins were identified from among the best matches under the constraints that the identity/similarity must lie within the N-terminal end and must have a molecular mass similar to the estimated mass derived from the mobility of protein in SDS-PAGE. For example, identification of the ~70-kDa protein in degradosomal fraction of *P. syringae* Lz4W as RhIE (PSPTO5070) homologue of *P. syringae* pv. tomato (25) was based not only on the identity of N-terminal amino acid sequence but also on its size (629 amino acids long), because another homologue, PSPTO4664, had an almost identical N-terminal amino acid sequence but was only 442 amino acids long.

**Purification of Recombinant Proteins from E. coli and Antibody Production**—The *P. syringae* RNase R gene (*rnr*) was amplified by the forward primer (5'-ATGGCCGATT-GGCAAACCTCGAT-3') and the reverse primer (5'-TCATGACTTGGCCTTAGG-3') from genomic DNA. The 2.651-kb PCR product was first cloned into the EcoRV site of the pMOSBlue plasmid (Amersham Biosciences). Then the *rnr* gene was cloned between the Sall and EcoRI sites of the expression vector pET28a (Novagen) to generate pETrnr-his producing N-terminal His-tagged RNase R protein. For RhIE, a part of the *rhIE* gene was ampli-

fied from *P. syringae* genomic DNA by PCR, using forward and reverse (5'-ATGCTCTTTKCTTCCTCGG-3' and 5'-CCGATGCGGTGSACRT-AGTCTTC-3') primers, respectively. The amplified fragment (~1 kb) encodes a truncated protein corresponding to the amino acid positions 1–340 of RhIE (PSPTO5070) in *P. syringae* pv. tomato (NCBI accession number NC004578.1). It was cloned into the pET28a expression vector. The successful cloning in-frame was confirmed by DNA sequencing. Both His-tagged recombinant proteins were expressed by isopropyl 1-thio- $\beta$ -D-galactopyranoside induction in *E. coli* BL21(DE3) and purified under denaturing conditions by Ni-NTA-agarose chromatography (Qiagen). The identity of the purified recombinant RNase R was additionally confirmed by N-terminal sequencing. The purified truncated His-tagged protein RhIE\* has a calculated molecular mass of ~40 kDa. The polyclonal antibodies were raised in rabbit against the purified recombinant RNase R and in mouse against the RhIE\* by using standard protocols. The anti-RhIE\* antibodies cross-reacted only to the degradosomal fraction-associated 70-kDa protein, confirming the identity of the expressed open reading frame as RhIE (PSPTO5070 homologue).

**Expression of His-tagged RNase E and RNase R in P. syringae**—For expression of His-tagged RNase E and RNase R in *P. syringae*, the *rne* and *rnr* genes were cloned into the broad host range plasmid vector pGL10 (26) to generate pGLrne-his and pGLrnr-his (details of cloning and expression will be published elsewhere). Briefly, the *rne* gene was amplified by PCR using primers (FPn1, 5'-ATGAAAAGAATGCTGAT-TAACGCAAC-3', and RP2, 5'-TCAGACGAGGGGTTTGGGCTGGT-GTTC-3') and was cloned in the EcoRV site of pMOSBlue (Amersham Biosciences). The gene was then ligated in-frame between the EcoRI and Sall sites of the expression vector pET28a (Novagen) to produce pETrne-his, similar to pETrnr-his described above. Subsequently, His-tagged *rne* and *rnr* reading frames were cleaved out as XbaI fragments from the respective pET28a expression vectors and were ligated into the XbaI site of the broad host range plasmid vector pGL10 (26). The constitutive expression from the *lacZ* promoter of the plasmid resulted in production of soluble His-tagged proteins, which were purified under native conditions using Ni-NTA-agarose (Qiagen) chromatography following the supplier's instructions.

**Analysis of Interacting Proteins by Ni-NTA Resin**—For analyzing interacting proteins, purified His-tagged RNase E (15–20  $\mu$ g) was mixed with SP-Sephacrose-eluted fraction (100–125  $\mu$ g of protein) of cell lysate from *P. syringae* in a buffer that contained 50 mM sodium phosphate, pH 8.0, 300 mM NaCl, and 20 mM imidazole. The mixture was incubated for 2 h at 4 °C by gentle shaking, and then 200  $\mu$ l of Ni-NTA slurry (50%) was added to it and incubated for another 1 h. The whole slurry was then processed for routine Ni-NTA-agarose chromatography, except that the column was washed with at least 10 volumes of phosphate buffer containing 60 mM imidazole. Resin-bound proteins were finally eluted with 250 mM imidazole. As a control, RNase treatment was performed prior to elution.

**Western Blot Analysis**—Western blotting was carried out following transfer of the separated proteins onto Hybond-C membrane (Amersham Biosciences) by a Bio-Rad semidry transfer apparatus. The membrane filters were probed with antisera raised against *R. capsulatus* RNase E (13) or *P. syringae* RNase R and RhIE (this work). The detection was performed using alkaline phosphatase-conjugated secondary anti-rabbit or anti-mouse goat IgG and standard protocols. A commercially available anti-His polyclonal antibody (Santa Cruz Biotechnology) was used to confirm expression of His-tagged proteins.

**Co-immunoprecipitation Experiments**—For co-immunoprecipitation experiments by anti-RNase R antibodies, 250  $\mu$ l of the SP-Sephacrose fraction (~125  $\mu$ g of protein) of *P. syringae* was incubated with 10  $\mu$ l of the antisera by gentle shaking for 2 h at 4 °C. Then 10  $\mu$ l of protein A-conjugated CL-agarose slurry (Bangalore Genei, India) was added and incubated further for 1 h. Protein A-agarose beads were then pelleted down by centrifugation (1500  $\times$  g, 2 min) and washed three times with buffer A (see protein fractionation method) containing 1 M NaCl. Finally, the agarose beads were resuspended in 100  $\mu$ l of sample loading buffer of SDS-PAGE. Following SDS-PAGE separation, the proteins were visualized by silver staining or processed for Western analysis. As a control, RNase treatment of SP fraction was performed prior to incubation with antibodies.

**In Vitro Transcription of RNAs and Enzyme Assays**—*In vitro* transcription using T7 RNA polymerase and purification of the [ $\alpha$ -<sup>32</sup>P]UTP-labeled pZBP transcript (27) on denaturing gels was performed as described (28, 29). When RNA I.26 was used, the plasmid pT7-R25 (a kind gift from Dr. J. G. Belasco) was used as template (30). Synthetic poly(A) substrate (Amersham Biosciences) was 5'-end-labeled with [ $\gamma$ -<sup>32</sup>P]ATP. Radioactively labeled RNA I.26 and poly(A) were purified from unincorporated nucleotides by Sephadex G-50 chromatography.

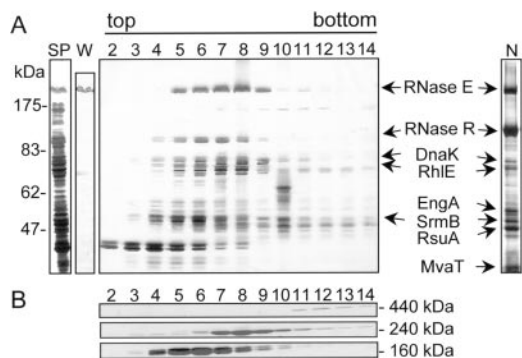


**FIG. 1. *P. syringae* RNase E co-sediments with RNase R in glycerol density gradients.** A, fractionation of pooled sulfopropyl-Sepharose (SP) fractions, which contain the 200-kDa RNase E polypeptide, through 10–30% glycerol density gradient. Aliquots of each fraction were resolved by SDS-PAGE and detected by silver staining. Lanes 2–14, glycerol density gradient fractions 2–14 (from the top to the bottom). Proteins identified by N-terminal sequencing are marked with arrows (the preparation shown in lane N was used for the protein identification). Lane W, Western blot analysis of the SP fraction with antibodies directed against RNase E of *R. capsulatus*. B, sedimentation behavior of marker proteins (ferritin, 440 kDa; catalase, 240 kDa; aldolase, 160 kDa) during centrifugation in 10–30% glycerol density gradients. Aliquots of each fraction were resolved by SDS-PAGE and detected by silver staining. Lanes 2–14, glycerol gradient fractions 2–14 from the top to the bottom. The migration behavior of the marker proteins (in kDa) is indicated.

The RNA degradation assays were performed in a buffer consisting of 25 mM Tris-HCl, pH 8.0, 5 mM MgCl<sub>2</sub>, 60 mM KCl, 100 mM NH<sub>4</sub>Cl, 0.5 mM dithiothreitol, 5% glycerol, in presence of RNasin (Promega). Optionally, this buffer was amended with 10 mM K<sub>2</sub>HPO<sub>4</sub> (for the PNPase assay) or with 5 mM ATP (for the helicase assay). The assays were performed in a final volume of 10  $\mu$ l with RNase E fractions containing 5 ng of *P. syringae* RNase R or 5 ng of *E. coli* PNPase (as determined by silver staining), His-tagged *P. syringae* RNase R, or His-tagged *P. syringae* RNase E. The reactions were terminated with 10  $\mu$ l of 10 mM Tris-HCl, pH 7.5, 10 mM EDTA, 0.2% SDS, and 1 mg/ml proteinase K and were incubated for 10 min at 50  $^{\circ}$ C. One sample was stopped immediately (time point 0). Generated RNA fragments were then detected by PhosphorImaging (Bio-Rad and Fuji).

**Polyadenylation of RNA for Degradation Assay**—To examine the effect of polyadenylation of RNA on degradation by exonucleases, the <sup>32</sup>P-labeled RNA I.26 was polyadenylated by *E. coli* poly(A) polymerase, PAP-I (Invitrogen) at 37  $^{\circ}$ C in presence of [ $\alpha$ -<sup>32</sup>P]ATP according to the supplier's instruction, and purified by NucAway spin column (Ambion). Both polyadenylated and control RNA I substrates were then assayed for degradation in the presence of purified RNase R and degradosomal fractions from glycerol gradients as described above.

**Thin Layer Chromatography**—*In vitro* degradation reaction mixtures were applied in two 5- $\mu$ l portions to a layer of Cellulose MN 300 PEI (Macherey & Nagel). After drying, the separation of uridine tri-, di-, and monophosphate was carried out using 0.9 M guanidine chloride, pH 6.3. The plate was dried and exposed to a PhosphorImager screen.

## RESULTS

***P. syringae* RNase R Is in a Complex with RNase E and RhIE**—To enrich *P. syringae* RNase E with associated proteins, we used the procedure already successfully applied for isolation of the RNase E-based protein complexes of *E. coli* and *R. capsulatus*. After ammonium sulfate precipitation of the 100,000  $\times$  g supernatant fraction and cation exchange chromatography, fractionation through a glycerol density gradient in the presence of protease inhibitors was performed. The protein content of the fractions was analyzed in SDS-PAGE (Fig. 1A). In parallel, the sedimentation behavior of marker proteins was monitored (Fig. 1B). In Fig. 1A, a protein band of ~200 kDa was detected in the 5–9 fraction from the top of the glycerol density gradient. This band showed a cross-reaction with antibodies specific for RNase E of *R. capsulatus* (lane W in Fig. 1A). The 118-kDa RNase E of *R. capsulatus* and *E. coli* mi-

grates in SDS-PAGE like a 180-kDa protein (1, 13). The *rne* gene of *P. syringae* DC3000 (NCBI accession number 28870994) encodes a protein of ~120 kDa. We concluded that the 200-kDa band in Fig. 1A represents aberrantly migrating RNase E of *P. syringae* Lz4W. This assumption was confirmed by N-terminal sequencing. To test the RNase E-containing fractions for an endoribonucleolytic activity, assays with labeled RNA substrates were performed in buffer devoid of inorganic phosphate. Most surprisingly, we observed strong hydrolytic exoribonuclease activity (see Fig. 4). This prompted us to identify other proteins in the RNase E-containing fractions by N-terminal sequencing. We found that RNase R, DnaK, RhIE, EngA, SrmB, RsuA, and MvaT homologues are present in the RNase E-containing fractions (Fig. 1A and Table I). The identification of homologues of two DEAD-box helicases (RhIE and SrmB) and an exoribonuclease (RNase R) in the RNase E fractions suggested that these fractions may contain the degradosome of *P. syringae*. This part of the glycerol density gradient (Fig. 1A, lanes 5–9) corresponds to proteins with a native molecular mass of 160–240 kDa (Fig. 1B). Thus, not all of the proteins present in the fractions 5–9 of the glycerol density gradient are in a complex. Only the amount of EngA was reduced in the RNase E fractions of glycerol gradient after RNase treatment of the SP fraction (data not shown).

In *E. coli*, the hydrolytic RNase R is important for rRNA degradation and transfer/messenger RNA maturation (22, 31). Involvement of RNase R with other proteins and/or RNA in a putative ribosome rescue complex has also been discussed (32), but its interaction with the degradosome organizer RNase E was not known until now. Instead, RNase E was shown to co-purify with PNPase (1–5, 12, 13). We decided to test whether RNase E and RNase R of *P. syringae* interact with each other, because they peaked in the same glycerol density gradient fractions (Fig. 1A). To this end, co-immunoprecipitation was performed with RNase R-directed antibodies and the RNase E-containing SP fraction of *P. syringae* (the cation exchanger fraction pool usually used for further glycerol gradient fractionation; see lane SP in Fig. 1A). In addition to RNase R, a 200-kDa polypeptide was specifically co-precipitated, which interacts with antibodies directed against RNase E of *P. syringae* (lanes IP in Fig. 2, A and B). The specificity of the co-precipitation of the 70-kDa polypeptide (most probably RhIE; lane IP in Fig. 2A) may be questioned because proteins of similar size interact with the preimmune serum (lane C in Fig. 2A).

To confirm further the interaction between RNase E and RNase R, His-tagged RNase E was purified under native conditions and incubated with the SP fraction. Ni-NTA pull-down was performed to isolate the recombinant RNase E together with the interacting proteins (Fig. 3A). Three additional polypeptide bands showed the same elution profile as the His-tagged RNase E. The two of them were identified as RNase R and RhIE by Western blot analysis (Fig. 3, B and C). A control experiment with the SP fraction from wild type *P. syringae* cells revealed that the polypeptide marked with C (Fig. 3A) sticks to the Ni-NTA resin and is not an RNase E-interaction partner (not shown). Another protein band was also enriched in the last elution fractions (marked with a question mark in Fig. 3A). Because the elution profile of this polypeptide was different from the RNase E elution profile, it was not investigated further. The results shown in Figs. 2 and 3 demonstrate that RNase E and RNase R interact with each other in *P. syringae* and that RhIE is also part of the protein complex.

**Functional Characterization of *P. syringae* Protein Fractions Comprising RNase E, RNase R, and RNA Helicases**—Previously, the endonucleolytic RNase E activity of *E. coli* and *R. capsulatus* degradosomes was demonstrated by their incu-

TABLE I  
*P. syringae* proteins that were co-purified by glycerol density gradient centrifugation

The proteins were identified by comparison of the N-terminal sequences with the data from *P. aeruginosa* genome project (www.pseudomonas.com) and recent genome sequence data of the *P. syringae* pv. *tomato* (25), known by their PA or PSPTO numbers, respectively.

Co-purified proteins	Apparent molecular mass	N-terminal sequence	Homology to (NCBI entry no.)	Function
	<i>kDa</i>			
RNase E	210	MKRMLINATQXEEL	PA2976/PSPTO3841	Endoribonuclease
RNase R	100	ADXQTLDPAAAREA	PA4937/PSPTO4935	Exoribonuclease
DnaK	75	MRIIGIDLGTNSCV	PA 4761/PSPTO4505	Chaperone
RhIE	70	RWASLGLSEALVRAF	PA0428/PSPTO5070	DEAD-box RNA helicase
EngA	52	MVPVIALVGRPNVGD	PA3799/PSPTO1438	GTPase
SrmB	51	MFLDFALHERLLAV	PA 3466/PSPTO1587	DEAD-box RNA helicase
RsuA	48	SDLDPKDSQEIGPAG	PA0733/PSPTO4247	Pseudouridine synthetase
AlgP	46	SANKKPVNTPLHLQ	PA5253/PSPTO0136	Transcriptional regulator
MvaT	40	MSLIAEYRAAEEAXGE	PA4315/PSPTO4315	Transcriptional regulator

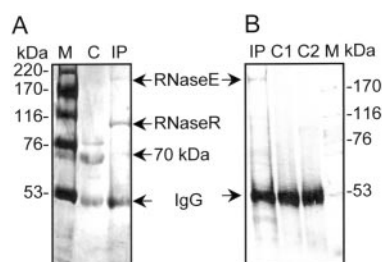


FIG. 2. Co-immunoprecipitation of RNase R and RNase E by antibodies directed against *P. syringae* RNase R. A, anti-RNase R antibodies were first incubated with the SP fraction of *P. syringae*. RNase R and RNase R-bound proteins were then isolated by protein A-conjugated agarose and analyzed by SDS-PAGE and silver staining (lane IP). Detected proteins are marked with arrows. C, control lane with the proteins that were precipitated with the pre-immune serum. B, Western blot analysis with antibodies directed against *R. capsulatus* RNase E. IP, proteins that were co-immunoprecipitated with anti-RNase R antibodies. C1, control lane showing the mock immunoprecipitation (corresponds to lane C in A). C2, anti-RNase R immune serum and protein A-conjugated agarose alone. M, protein marker (in kDa).

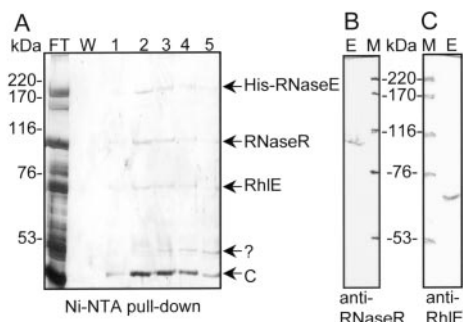


FIG. 3. Ni-NTA pull-down of RNase E, RNase R, and RhIE of *P. syringae*. A, His-tagged RNase E of *P. syringae* was incubated with the SP fraction. The recombinant RNase E and interacting proteins were isolated by Ni-NTA pull down and analyzed by SDS-PAGE and silver staining. Lane FT, flow-through; lane W, last washing fraction; lanes 1-5, elution fractions. Detected proteins are marked with arrows. The migration behavior of marker proteins (in kDa) is indicated. B, Western blot analysis of elution fraction 2 (lane E) by anti-RNase R antibodies. C, Western blot analysis of elution fraction 2 (lane E) by anti-RhIE antibodies. M, protein marker (in kDa).

bation with suitable RNA substrates in the absence of phosphate ions. Under these conditions, the products of endonucleolytic cleavage were detectable, because the phosphate-dependent PNPase could not degrade them exonucleolytically (1, 13). To test for RNase activity, the *P. syringae* RNase E-containing fraction shown in Fig. 4A (lane Ps) was incubated with internally labeled RNA in the absence and in the presence of phosphate. In parallel, the assays were performed with the *E. coli* degradosome fraction shown in Fig. 4A (lane Ec). As a substrate, [ $\alpha$ -<sup>32</sup>P]UTP-labeled pZBP transcript derived from

the *R. capsulatus* *puf* operon, which can be cleaved by *E. coli* and *R. capsulatus* RNase E was used (27). The cleavage products were analyzed by electrophoresis (Fig. 4B) and by thin layer chromatography (Fig. 4C).

As shown in Fig. 4B, the *P. syringae* fraction degraded RNA without accumulation of intermediate cleavage products in the presence and absence of phosphate (lanes 1-4). As an end product, a band that could represent UMP was detected. Because of its charge, UMP migrates more slowly in SDS gels than the UTP marker. This is consistent with the presence of RNase R, an exoribonuclease with a hydrolytic mode of action (33), in the RNase E-containing protein fraction of *P. syringae*.

As expected, the *E. coli* protein fraction produced distinct cleavage products in the absence of phosphate (Fig. 4B, lanes 5 and 7). A prominent 171/165-nucleotide band, which also arises by cleavage of this substrate with degradosome fractions of *R. capsulatus* (13), is marked in Fig. 4B. In the presence of phosphate, these products of endonucleolytic cleavage were not detected, because of phosphorolytic degradation by the exoribonuclease PNPase. Based on its migration, the final RNA degradation product could represent UDP (Fig. 4B, lanes 6 and 8).

The phosphorolytic degradation of RNA by PNPase results in production of nucleoside diphosphates (1), whereas its hydrolytic degradation by RNase R should lead to generation of nucleoside monophosphates (33). To confirm the hydrolytic activity in the *P. syringae* protein fraction, thin layer chromatography analysis of the radioactive mononucleoside products of the exoribonucleolytic reaction was performed (Fig. 4C). The incubation of internally labeled RNA with the *P. syringae* protein fraction in the presence or in absence of phosphate resulted in the generation of uridine monophosphate. This is consistent with hydrolytic RNA degradation by RNase R (Fig. 4C, lanes 1-3). As expected, PNPase in the *E. coli* degradosome generated uridine diphosphate in the presence of phosphate in the buffer (Fig. 4C, lanes 5 and 6). This reaction did not occur in buffer devoid of phosphate (Fig. 4C, lane 4). The results of this experiment confirmed the presence of a hydrolytic exoribonuclease instead of a phosphorolytic one in the *P. syringae* RNase E-containing fraction.

According to the results shown in Fig. 3, the RNase E-RNase R protein complex interacts with the RhIE homologue in *P. syringae*. Therefore, we decided to test RNase E-containing fractions for RNA helicase activity, keeping in mind that a second putative RNA helicase, the SrmB homologue, is also present in these fractions (Fig. 1A). The helicase assay is based on the observation that exoribonucleases stop RNA degradation when encountering stable, double-stranded structures. The exonucleolytic RNA degradation can proceed if RNA helicases unwind the hairpin structures upon ATP hydrolysis (2). Thus, the helicase assay can be performed only if RNase R

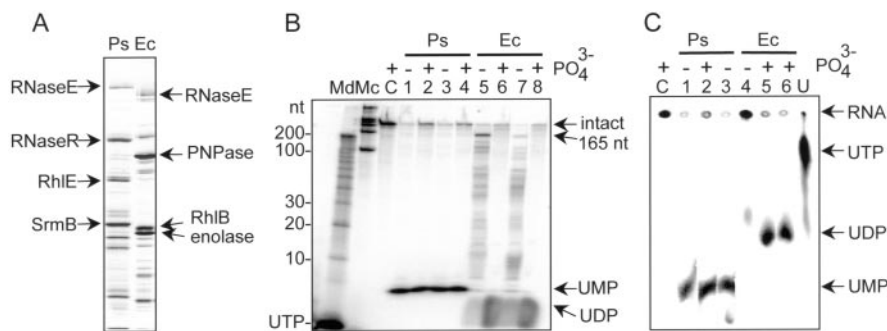


**FIG. 4. RNase E-containing glycerol density gradient fraction of *P. syringae* shows hydrolytic exoribonuclease activity.** *A*, silver-stained SDS gel showing proteins from RNase E-containing glycerol density gradient fractions of *P. syringae* (Ps) and *E. coli* (Ec). Relevant proteins are marked with arrows. *B*, phosphorimager of urea-polyacrylamide gel showing RNA degradation assays at 22 °C. Internally labeled pZBP transcript (13) and the *P. syringae* (Ps) or the *E. coli* (Ec) protein fraction shown in *A* were used. The presence or absence of phosphate is indicated on the top. Lanes 1, 2, 5, and 6, incubation for 5 min; lanes 3, 4, 7, and 8, incubation for 10 min. Lane C, negative control, transcript incubated in buffer for 10 min. Md, RNA decade marker; Mc, RNA century marker (Ambion). The migration of the marker molecules in nucleotides (nt) is marked. The migration of the intact transcript (intact), of major 171/165-nucleotide RNase E cleavage products (165 nt) (13), and of the final products (UMP and UDP) is marked by arrows. *C*, thin layer chromatography analysis of RNA degradation assays as described in *B*. Lane C, negative control; lanes 1, 2, 4, and 5, incubation for 5 min; lanes 3 and 6, incubation for 10 min; U, UTP was loaded. The migration position of UTP, UDP, and UMP is marked with arrows. RNA indicates the substrate and endonucleolytic products, which are not resolved by this technique.

cannot efficiently proceed through double-stranded RNA. So far, only RNase R of *E. coli* was characterized (31, 33). This enzyme can degrade ribosomal RNA *in vitro* in the absence of helicases, but RNase R-mediated exonucleolytic degradation stops at double-stranded structures in other RNA substrates (33). Therefore, it seemed possible to perform RNA helicase activity assays using the RNA I.26 substrate. RNA I.26 is an untranslated regulatory RNA that controls the replication of ColE1-type plasmids such as pBR322 and contains stem-loops and an RNase E cleavage site (Fig. 5A) (30).

The result of the assay is shown in Fig. 5B. The RNA I.26 substrate consists of RNAs with length of 130 (short (S)) and 185 nucleotides (long (L)), which are generated during the *in vitro* transcription. These RNA species contain an RNase E cleavage site at position 27 (Fig. 5A) (30). Cleavage of the transcripts L and S by RNase E of *P. syringae* leads to the appearance of the bands  $C_L$  and  $C_S$ , respectively (Fig. 5, A–C). In the presence of ATP, the full-length transcripts and the RNase E cleavage products were continuously degraded by the *P. syringae* fraction (Fig. 5B). In the absence of ATP, the transcript S was fully converted to  $C_S$  by RNase E, and this cleavage product remained stable, probably due to the hairpin structures at its 3'-end, which blocked further degradation by RNase R (Fig. 5, A and B). The transcript L was cleaved only partially at the RNase E site during the incubation period of the experiment. The remaining L transcript and its cleavage product  $C_L$  were not efficiently degraded in the absence of ATP (Fig. 5B). Obviously, the 3'-end of these RNAs adopts secondary structures, which cannot be degraded by *P. syringae* RNase R. This was confirmed by incubation of RNA I.26 in the presence of a purified recombinant RNase R of *P. syringae* (Fig. 5D). The His-tagged RNase R was not able to degrade this substrate, although it showed exonucleolytic activity on 5'-end-labeled and single-stranded poly(A) (Fig. 5E).

The result shown in Fig. 5B allows two different interpretations. On the one hand, the strong RNA degradation in the presence of ATP may be due to the unwinding of double strand RNA structures by the RhlE and SrmB homologues in the used *P. syringae* protein fraction. On the other hand, the RNA degradation in the presence of ATP may also be due to polyadenylation of the substrate by an uncharacterized enzyme, such as PAP that might be present in the protein fraction. Polyadenylated RNAs are efficiently degraded by bacterial exoribonucleases (34). To verify the latter possibility, the RNA I.26 was polyadenylated *in vitro* with *E. coli* PAP I and then treated

either with purified recombinant His-tagged RNase R (not shown) or with RNase E-containing glycerol gradient fraction of *P. syringae*, in the absence of ATP (Fig. 6A). The polyadenylated substrate (RNA I.26-poly(A)) had slower mobility in the gel because of the presence of poly(A) tails of 12–25 nucleotides (Fig. 6B). The results (Fig. 6A) indicate that polyadenylation did not facilitate the degradation of the substrate. Therefore, the PAP activity, if present in the *P. syringae* degradosome fraction, was unlikely to be responsible for the decay of RNA I.26 in presence of ATP (Fig. 5B). It is more likely that the helicase activity associated with the fraction is responsible for unwinding of the stem-loop structures of RNA I.26 in the presence of ATP, which makes the substrate amenable to exonuclease attack by RNase R. Because RhlE, but not SrmB, can be pulled down along with RNase R, by His-tagged RNase E (Fig. 3) it is also likely that RhlE acts as the helicase component of the RNase E-based degradosomal complex in the Antarctic *P. syringae*.

We also analyzed the variation in the components of the *P. syringae* degradosome-like complex under different growth conditions, following glycerol gradient fractionation of the proteins from *P. syringae* cells grown at 4 or 22 °C or incubated at 37 °C after growth at 22 °C. The protein composition of the glycerol gradient fractions of all three isolations was comparable, except that the amount of DnaK at 37 °C increased (not shown). Additionally, to examine the temperature optima of the enzyme activities in the complex in this low temperature-adapted bacterium, the activity assays were performed at 4, 22, and 37 °C. Remarkably, the enzymatic activities increased with the increasing assay temperature. The highest *in vitro* activity of the RNases and helicases was observed at 37 °C (data not shown) as seen for RNA polymerase from this bacterium (35).

## DISCUSSION

In this work, we show that in the Antarctic psychrotrophic strain *P. syringae* Lz4W RNase R interacts with RNase E. The DEAD-box helicase RhlE is also part of the protein complex. The association of RNase E with an exoribonuclease and an RNA helicase suggests that this protein complex constitutes the *P. syringae* degradosome. RNase E, RNase R, and RhlE had similar distribution in the glycerol density gradient, and their sedimentation corresponds to the sedimentation of proteins with a native molecular mass of ~160–240 kDa (Fig. 1). This may indicate the existence of dynamic sub-complexes, which may

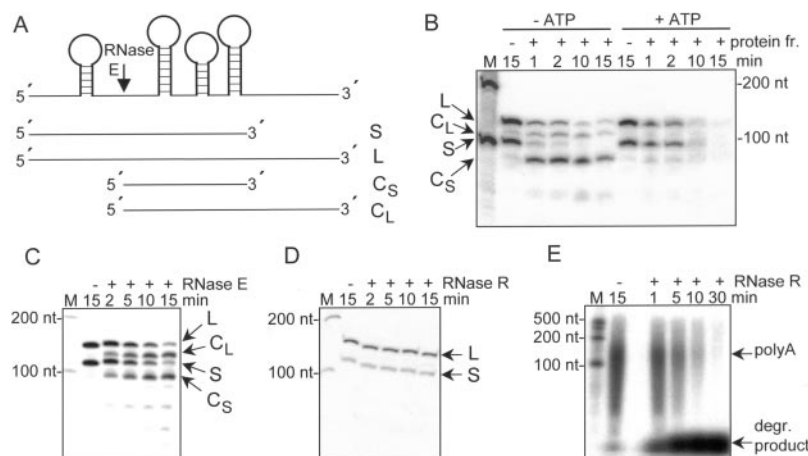


**FIG. 5. ATP promotes the exonucleolytic degradation of the structured RNA I.26 transcript by the RNase E-containing glycerol density gradient fractions of *P. syringae*.** *A*, schematic representation of the stem-loop containing RNA I.26 (30). The short (*S*) and long (*L*) transcripts arise because of an intrinsic termination and run-off transcription from the linearized plasmid template. Processing at the RNase E cleavage site 27 bases from the 5'-end results in the cleavage products  $C_L$  and  $C_S$ . *B–E* show phosphorimages of urea-polyacrylamide gels. *B*, RNA degradation activity for indirect helicase assay in the presence or absence of ATP (indicated on the top) with RNA I.26 substrate and the *P. syringae* RNase E-containing glycerol gradient fraction (*protein fr.*). The fraction shown in lane *N* of Fig. 1A is representative for the protein samples used here. The incubation time is indicated (in min). *M*, RNA century marker (in nt, indicated at the right side of the panel). The migration of the *L* and *S* forms of the transcript and the corresponding RNase E cleavage products,  $C_L$  and  $C_S$ , are marked with arrows. *C*, cleavage of RNA I.26 by purified His-tagged RNase E of *P. syringae*. Descriptions as in *B*. Activity of purified His-tagged RNase R of *P. syringae* on RNA I.26 (*D*) and poly(A) (*E*) substrates are shown. Descriptions as in *B*; *degr. product*, degradation product.

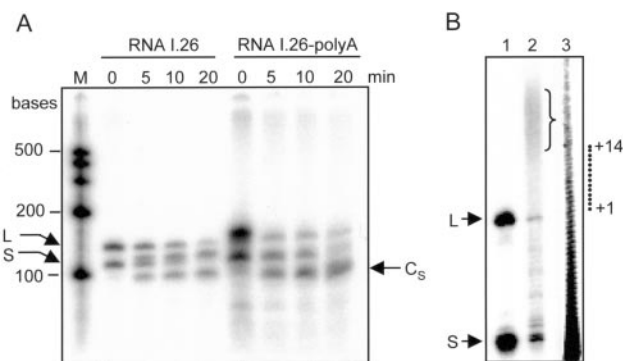


**FIG. 6. Degradation activity of RNase E-containing glycerol gradient fraction from *P. syringae* on polyadenylated RNA I.26 substrate.** *A*, RNA I.26 was polyadenylated with *E. coli* PAP I. Polyadenylated RNA I.26 (RNA I.26-poly(A)) and RNA I.26 were incubated with the degradosome fraction from glycerol gradient, in the absence of ATP for the indicated times. Both *L* and *S* forms of RNA I.26, RNase E cleavage product  $C_S$ , and the size of the RNA markers are indicated. *B*, size determination of poly(A) tails in an 8 M urea, 6% polyacrylamide sequencing gel. Lane 1, non-polyadenylated RNA I.26 substrate; lane 2, RNA I.26 substrate polyadenylated with *E. coli* PAP I; lane 3, poly(A) ladder. The *L* and *S* forms of non-polyadenylated RNA I.26 are indicated at the left side of the panel. The polyadenylated RNA I.26 molecules are marked with a brace in the panel. Poly(A) ladder molecules, which are 1–14 nucleotides longer than the *L* form of RNA I.26, are marked with dots at the right side of the panel.

consist of RNase E and RhlE, RNase R, and RhlE, or all three. The presence of other proteins in the same glycerol gradient is most probably co-incident. The pull-down of RNase E together with RNase R and RhlE from such fractions indicates that these three proteins interact with each other, at least transiently, to make a complex, which is not bound by RNA. The distribution of the degradosomes of *E. coli* (1) and *R. capsulatus* (13) in glycerol density gradients also suggests the existence of (transient) sub-complexes. So far, all analyzed degradosomes of *E. coli* (1), *R. capsulatus* (13), and *P. syringae* (this work) show sedimentation behavior, which is not consistent with the presence of a tetrameric RNase E, although it was shown that the conserved catalytic domain of *E. coli* RNase E forms a homotetramer (36). However, it was recently demonstrated that the C-terminal domain of RNase E is intrinsically unstructured and is unlikely to

be extensively folded within the degradosome (37). If the C-terminal domain of RNase E acts as a flexible tether of the degradosome complex, its sedimentation behavior may be very different from that of the marker proteins.

The *P. syringae* degradosome contains a hydrolytic exoribonuclease activity (RNase R) instead of the phosphorolytic one (PNPase) like in *E. coli*. So far, only the phosphate-dependent exonuclease PNPase was shown to be part of the *E. coli* degradosome (1), to interact with RNase E of *S. coelicolor* (12), or to co-purify with the *R. capsulatus* degradosome in substoichiometric amounts (13). Eukaryotic exosomes were also found to contain PNPase-like proteins (14, 15), indicating the evolutionary conservation of phosphorolytic activities in the two protein complexes. The composition of the *P. syringae* RNA-degrading complex suggests that the bacterial degradosomes must not always contain PNPase.

The physical association between RNase E, RNA helicase, and a hydrolytic or phosphorolytic exoribonuclease is a common theme in all bacterial degradosomes. Hydrolytic and phosphorolytic exoribonucleases as well as RNA helicases are also parts of the eukaryotic exosome (38, 39). The mitochondrial degradosome (mtEXO) also contains a hydrolytic RNase II-like exoribonuclease and an RNA helicase (40). Such complexes have not been detected so far in chloroplasts (41), although the combined action of endo- and exoribonucleases is required for RNA processing and degradation in these organelles (42). Protein interaction studies indicated that PNPase of *E. coli* can interact with the DEAD-box helicase RhlB. Therefore, it was proposed that a separate mini-complex of PNPase and RhlB may exist in parallel to the degradosome (43). On the other hand, the interaction between RhlB and PNPase of *E. coli* is not very strong (43) and was not detected by other groups (3, 44). Moreover, it was shown that the association of RhlB and PNPase with RNase E as degradosome components is required for *in vivo* degradation of structured RNA fragments (9). However, it cannot be excluded that the interaction of enzymes that are involved in RNA processing and degradation undergoes dynamic changes to produce different complexes, which might be important for adaptive cellular functions.

The sequenced genome of *P. syringae* DC3000 (25) contains genes for at least five DEAD-box RNA helicases including

RhlB (PSPTO1253), CsdA/DEAD (PSPTO1775), RhlE (the following two homologues: larger (PSPTO5070) and smaller (PSPTO4664)), and SrmB (PSPTO1587). The larger RhlE homologue and SrmB were detected in the *P. syringae* glycerol density gradient fractions that consist of RNase E and RNase R, but only the RhlE was shown to co-purify with these RNases in the pull-down experiments. *E. coli* also contains five different DEAD-box proteins including SrmB, RhlB, CsdA, and RhlE, and their particular functions are not clear (45). So far only RhlB was identified as a part of the *E. coli* degradosome (2–5). Only the RhlE out of three *E. coli* DEAD-box helicases (RhlE, CsdA, and SrmB) can effectively unwind RNA duplexes when single-stranded RNA extensions are short or absent (46). SrmB and CsdA were shown to be involved in the biogenesis of the large ribosomal subunit (47, 48). Most interestingly, SrmB and RhlE, as well as RNase E, can interact with poly(A) polymerase in *E. coli* (7) where polyadenylation of RNA leads to its destabilization (49). Thus, the data from *E. coli* (7, 49) imply that SrmB and RhlE may participate in RNA degradation. Our finding that in *P. syringae* RhlE interacts with RNase E and RNase R confirms this assumption.

*P. syringae* Lz4W contains genes for both RNase R and PNPase, and PNPase is expressed in this bacterium.<sup>2</sup> Why then has RNase R been selected for the RNase E-based degradosome in the psychrotrophic *P. syringae*? It is now established that in mesophilic *E. coli*, PNPase and RNase R accumulate under cold shock, but PNPase is essential at low temperatures (22, 23, 50). Also in the psychrotrophic *Yersinia enterocolitica*, the PNPase is essential for growth at low temperature (51). However, in *Pseudomonas putida* the physiological role of PNPase seems to be different; a PNPase-deficient mutant of *P. putida* is not cold-sensitive (52). RNase R, on the other hand, is important for rRNA quality control in *E. coli*. The enzyme can degrade rRNA even in the absence of helicases (31). A high processivity of RNase R through the secondary structures of RNA might be one reason for its recruitment in the complex with RNase E in the degradosome of the psychrotrophic bacterium, which would allow conserving energy (ATP) during growth at low temperature. Most interestingly, very fast rRNA degradation occurs in *P. syringae* Lz4W at supraoptimal temperatures (53). It is possible that a degradosome comprising RNase R can participate more efficiently in rRNA degradation than the PNPase-containing *E. coli* degradosome, which is involved in rRNA turnover (54). The fact that the *rnr* gene is present even in the minimal *Mycoplasma* genome and can be found in more bacterial genomes than the *pnp* gene (33, 55) suggests that RNA-degrading complexes containing RNase R may exist in other bacteria.

**Acknowledgments**—We thank Prof. J. G. Belasco for the plasmid pT7-R25, M. Sultana for oligonucleotide synthesis, N. Nagesh for DNA sequencing, and animal laboratory facility at Centre for Cellular and Molecular Biology for help in raising antibodies.

#### REFERENCES

- Carpousis, A. J., Van Houwe, G., Ehretmann, C., and Krisch, H. M. (1994) *Cell* **76**, 889–900
- Py, B., Higgins, C. F., Krisch, H. M., and Carpousis, A. J. (1996) *Nature* **381**, 169–172
- Vanzo, N. F., Li, Y. S., Py, B., Blum, E., Higgins, C. F., Raynal, L. C., Krisch, H. M., and Carpousis, A. J. (1998) *Genes Dev.* **12**, 2770–2778
- Sohlberg, B., Lundberg, U., Hartl, F. U., and von Gabain, A. (1993) *Proc. Natl. Acad. Sci. U. S. A.* **90**, 277–281
- Miczak, A., Kaberdin, V. R., Wei, C. L., and Lin-Chao, S. (1996) *Proc. Natl. Acad. Sci. U. S. A.* **93**, 3865–3869
- Blum, E., Py, B., Carpousis, A. J., and Higgins, C. F. (1997) *Mol. Microbiol.* **26**, 387–398
- Raynal, L. C., and Carpousis, A. J. (1999) *Mol. Microbiol.* **32**, 765–775
- Liou, G. G., Jane, W. N., Cohen, S. N., Lin, N. S., and Lin-Chao, S. (2001) *Proc. Natl. Acad. Sci. U. S. A.* **98**, 63–68
- Khemici, V., and Carpousis, A. J. (2004) *Mol. Microbiol.* **51**, 777–790
- Bernstein, J. A., Lin, P. H., Cohen, S. N., and Lin-Chao, S. (2004) *Proc. Natl. Acad. Sci. U. S. A.* **101**, 2758–2763
- Kaberdin, V. R., Miczak, A., Jakobsen, J. S., Lin-Chao, S., McDowall, K. J., and von Gabain, A. (1998) *Proc. Natl. Acad. Sci. U. S. A.* **95**, 11637–11642
- Lee, K., and Cohen, S. N. (2003) *Mol. Microbiol.* **48**, 349–360
- Jäger, S., Fuhrmann, O., Heck, C., Hebermehl, M., Schiltz, E., Rauhut, R., and Klug, G. (2001) *Nucleic Acids Res.* **29**, 4581–4588
- Symmons, M. F., Williams, M. G., Luisi, B. F., Jones, G. H., and Carpousis, A. J. (2002) *Trends Biochem. Sci.* **27**, 11–18
- Aloy, P., Ciccarelli, F. D., Leutwein, C., Gavin, A. C., Superti-Furga, G., Bork, P., Bottcher, B., and Russell, R. B. (2002) *EMBO Rep.* **3**, 628–635
- Evguenieva-Hackenberg, E., Walter, P., Hochleitner, E., Lottspeich, F., and Klug, G. (2003) *EMBO Rep.* **4**, 889–893
- Koonin, E. V., Wolf, Y. I., and Aravind, L. (2001) *Genome Res.* **11**, 240–252
- Cheng, Z. F., Zuo, Y., Li, Z., Rudd, K. E., and Deutscher, M. P. (1998) *J. Biol. Chem.* **273**, 14077–14080
- Lin-Chao, S., Wei, C. L., and Lin, Y. T. (1999) *Proc. Natl. Acad. Sci. U. S. A.* **96**, 12406–12411
- Kobe, T., Sasakawa, C., Okada, N., Honma, Y., and Yoshikawa, M. (1992) *J. Bacteriol.* **174**, 6359–6367
- Clements, M. O., Eriksson, S., Thompson, A., Lucchini, S., Hinton, J. C., Normark, S., and Rhen, M. (2002) *Proc. Natl. Acad. Sci. U. S. A.* **99**, 8784–8789
- Cairrao, F., Cruz, A., Mori, H., and Arraiano, C. M. (2003) *Mol. Microbiol.* **50**, 1349–1360
- Polissi, A., De Laurentis, W., Zangrossi, S., Briani, F., Longhi, V., Pesole, G., and Deho, G. (2003) *Res. Microbiol.* **154**, 573–580
- Janiyani, K. L., and Ray, M. K. (2002) *Appl. Environ. Microbiol.* **68**, 1–10
- Buell, C. R., Joardar, V., Lindenberg, M., Selengut, J., Paulsen, I. T. et al. (2003) *Proc. Natl. Acad. Sci. U. S. A.* **100**, 10181–10186
- Bidle, K. A., and Bartlett, D. H. (1999) *J. Bacteriol.* **181**, 2330–2337
- Fritsch, J., Rothfuchs, R., Rauhut, R., and Klug, G. (1995) *Mol. Microbiol.* **15**, 1017–1029
- Milligan, J. F., and Uhlenbeck, O. C. (1989) *Methods Enzymol.* **180**, 51–62
- Conrad, C., Rauhut, R., and Klug, G. (1998) *Nucleic Acids Res.* **26**, 4446–4453
- Jiang, X., Diwa, A., and Belasco, J. G. (2000) *J. Bacteriol.* **182**, 2468–2475
- Cheng, Z. F., and Deutscher, M. P. (2003) *Proc. Natl. Acad. Sci. U. S. A.* **100**, 6388–6393
- Karzai, A. W., and Sauer, R. T. (2001) *Proc. Natl. Acad. Sci. U. S. A.* **98**, 3040–3044
- Cheng, Z. F., and Deutscher, M. P. (2002) *J. Biol. Chem.* **277**, 21624–21629
- Coburn, G. A., and Mackie, G. A. (1998) *J. Mol. Biol.* **279**, 1061–1074
- Uma, S., Jadhav, R. S., Seshukumar, G., Shivaji, S., and Ray, M. K. (1999) *FEBS Lett.* **453**, 313–317
- Callaghan, A. J., Grossmann, J. G., Redko, Y. U., Ilag, L. L., Moncrieffe, M. C., Symmons, M. F., Robinson, C. V., McDowall, K. J., and Luisi, B. F. (2003) *Biochemistry* **42**, 13848–13855
- Callaghan, A. J., Aurikko, J. P., Ilag, L. L., Grossmann, J., Chandran, V., Kuhnel, K., Poljak, L., Carpousis, A. J., Robinson, C. V., Symmons, M. F., and Luisi, B. F. (2004) *J. Mol. Biol.* **340**, 965–979
- Allmang, C., Kufel, J., Chanfreau, G., Mitchell, P., Petfalski, E., and Tollervey, D. (1999) *EMBO J.* **18**, 5399–5410
- Tran, H., Schilling, M., Wirbelauer, C., Hess, D., and Nagamine, Y. (2004) *Mol. Cell* **13**, 101–111
- Dziembowski, A., Piwowarski, J., Hoser, R., Minczuk, M., Dmochowska, A., Siep, M., van der Spek, H., Grivell, L., and Stepien, P. P. (2003) *J. Biol. Chem.* **278**, 1603–1611
- Baginsky, S., Shteiman-Kotler, A., Liveanu, V., Yehudai-Resheff, S., Bellaoui, M., Settlege, R. E., Shabanowitz, J., Hunt, D. F., Schuster, G., and Gruissem, W. (2001) *RNA (N. Y.)* **7**, 1464–1475
- Bollenbach, T. J., Schuster, G., and Stern, D. B. (2004) *Prog. Nucleic Acids Res. Mol. Biol.* **78**, 305–337
- Liou, G. G., Chang, H. Y., Lin, C. S., and Lin-Chao, S. (2002) *J. Biol. Chem.* **277**, 41157–41162
- Coburn, G. A., Miao, X., Briant, D. J., and Mackie, G. A. (1999) *Genes Dev.* **13**, 2594–2603
- Kalman, M., Murphy, H., and Cashel, M. (1991) *New Biol.* **3**, 886–895
- Bizebard, T., Ferlenghi, I., Iost, I., and Dreyfus, M. (2004) *Biochemistry* **43**, 7857–7866
- Charollais, J., Pflieger, D., Vinh, J., Dreyfus, M., and Iost, I. (2003) *Mol. Microbiol.* **48**, 1253–1265
- Charollais, J., Dreyfus, M., and Iost, I. (2004) *Nucleic Acids Res.* **32**, 2751–2759
- Mohanty, B. K., and Kushner, S. R. (1999) *Mol. Microbiol.* **34**, 1094–1108
- Zangrossi, S., Briani, F., Ghisotti, D., Regonesi, M. E., Tortora, P., and Deho, G. (2000) *Mol. Microbiol.* **36**, 1470–1480
- Goverde, R. L., Veld, J. H. J., Kusters, J. G., and Mooi, F. R. (1998) *Mol. Microbiol.* **28**, 555–569
- Favaro, R., and Deho, G. (2003) *J. Bacteriol.* **185**, 5279–5286
- Ray, M. K., Sitaramamma, T., Kumar, G. S., Kannan, K., and Shivaji, S. (1999) *Curr. Microbiol.* **38**, 143–150
- Bessarab, D. A., Kaberdin, V. R., Wie, C. L., Liou, G. G., and Lin-Chao, S. (1998) *Proc. Natl. Acad. Sci. U. S. A.* **95**, 3157–3161
- Zuo, Y., and Deutscher, M. P. (2001) *Nucleic Acids Res.* **29**, 1017–1026

<sup>2</sup> R. I. Purusharth, F. Klein, S. Sulthana, S. Jäger, M. V. Jagannadham, E. Evguenieva-Hackenberg, M. K. Ray, and G. Klug, unpublished observations.